JOC The Journal of Organic Chemistry

Article

pubs.acs.org/joc

Biocatalytic Route to Chiral Acyloins: P450-Catalyzed Regio- and Enantioselective α-Hydroxylation of Ketones

Rubén Agudo,[†,‡,§] Gheorghe-Doru Roiban,[†,‡,§] Richard Lonsdale,[†,‡,§] Adriana Ilie,[†,‡,§] and Manfred T. Reetz*[,†,‡]

[†]Department of Chemistry, Philipps-Universität Marburg, Hans-Meerwein Strasse, 35032 Marburg, Germany

[‡]Max-Planck-Institut für Kohlenforschung, Kaiser-Wilhelm-Platz 1, 45470 Mülheim an der Ruhr, Germany

Supporting Information

ABSTRACT: P450-BM3 and mutants of this monooxygenase generated by directed evolution are excellent catalysts for the oxidative α-hydroxylation of ketones with formation of chiral acyloins with high regioselectivity (up to 99%) and enantioselectivity (up to 99% ee). This constitutes a new route to a class of chiral compounds that are useful intermediates in the synthesis of many kinds of biologically active compounds.

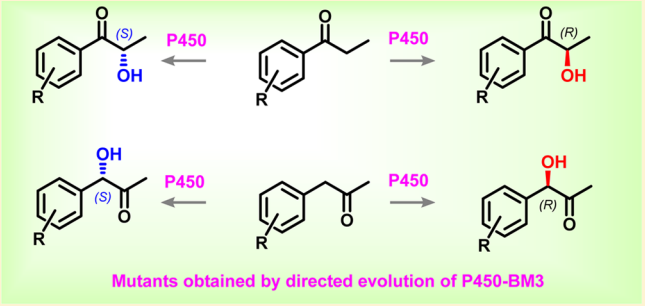

INTRODUCTION

Chiral α-hydroxyketones (acyloins) are useful building blocks in synthetic organic chemistry, and this functionality also occurs in a number of natural products and therapeutic drugs.[1] Due to the importance of this class of compounds, numerous approaches to their synthesis have been developed, utilizing a variety of strategies based on different starting materials, with catalytic asymmetric processes being of particular interest.[1] Prominent methods include α-hydroxylation of ketones or enolates by use of chiral transition metal catalysts[2] or organocatalysts,[3] benzoin condensation with chiral nucleophilic carbenes as catalysts,[4] and monooxidation of 1,2-diols.[5] Enzymes as mild and selective catalysts in synthetic organic chemistry constitute alternative strategies that are often complementary.[6] Several different biocatalytic approaches have been reported thus far for asymmetric acyloin formation:[1] carboligation of aldehydes catalyzed by thiamine diphosphate-dependent lyases,[7] reductase-catalyzed reduction of 1,2-diketones,[8] and oxidase-catalyzed oxidation of vicinal diols.[9] Moreover, lipase-catalyzed (dynamic) kinetic resolution of racemic acyloins and α-acetoxy ketones are also useful entries.[10] Finally, chiral allylic acetates, obtained by lipase-catalyzed dynamic kinetic resolution, have been subjected to Ru-catalyzed $NaIO_4$-based oxidation with formation of enantiomerically enriched acyloin acetates,[11a] and in one case desymmetrization of 3-phenylpenta-2,4-dione catalyzed by a Baeyer−Villiger monooxygenase provided the acylated form of the respective acyloin.[11b] These biocatalytic approaches all depend on different starting materials, which enables flexibility in synthesis planning.

RESULTS AND DISCUSSION

In the present study we report a new biocatalytic approach utilizing completely different starting compounds: namely, the regio- and enantioselective oxidative α-hydroxylation of ketones catalyzed by cytochrome P450 monooxygenases (CYPs).[12] By use of **1** as the ketone (Scheme 1), we discovered that wild-type (WT) P450-BM3 from *Bacillus megaterium*[13] enables the desired α-hydroxylation with essentially complete regioselectivity (99%) and fairly high enantioselectivity (89% ee) in favor of (*R*)-**2** being observed (Table 1, entry 1). Ketone **3** reacted with similar levels of regioselectivity (99%) and enantioselectivity (88% ee); in this case (*S*)-**4** is the favored product (Table 1, entry 15). These types of acyloins are precursors of various members of the ephedrine family.

In order to enhance but also to invert stereoselectivity in the formation of acyloin **2**, WT P450-BM3 was subjected to directed evolution[14] via structure-guided saturation mutagenesis at sites around the binding pocket (CASTing).[15] Three double-residue sites [A (V78/T88), B (V78/L181), and C (T268/A328)] and one single-residue site [D (F87)] surrounding the catalytic site were mutated (Supporting Information, Figure S1). The screening effort was reduced by randomizing double-residue sites with a highly reduced amino acid alphabet[15] composed of only six amino acids (Phe, Tyr, Trp, Lys, Arg, and His) and the corresponding WT, while NNK (N = adenine/cytosine/guanine/thymine; K = guanine/thymine) codon degeneracy was chosen for randomization of site D. In total, 760 transformants were screened, leading to several highly improved *R*-selective mutants with up to 99% regio- and 99% enantioselectivity (Table 1, entry 6). Only moderately *S*-selective mutants were found, namely, F87S and F87T [enantiomeric excess (ee) = 36% and 34%, respectively; Table 1, entries 8 and 9]. In order to

Received: October 28, 2014
Published: December 11, 2014

   dx.doi.org/10.1021/jo502397s | J. Org. Chem. 2015, 80, 950−956

Scheme 1. Oxidation of Ketones 1 and 3 by P450-BM3

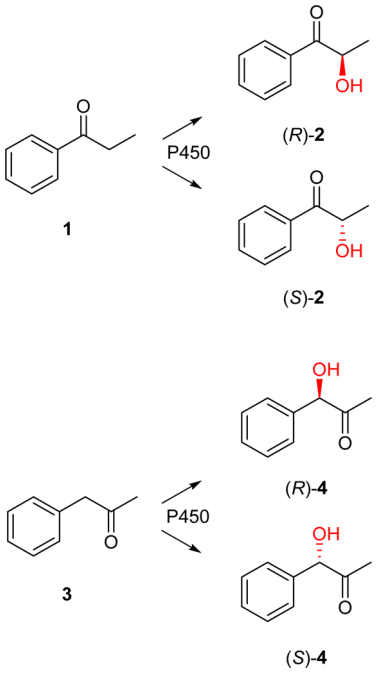

Table 1. Oxidative Hydroxylation of Ketones 1 and 3, Catalyzed by the Most Regioselective Mutants of P450-BM3.[a]

entry	substrate	P450-BM3	product	% regio	% ee
1	**1**	WT	(*R*)-**2**	99	89
2	**1**	V78F	(*R*)-**2**	98	94
3	**1**	V78H	(*R*)-**2**	99	96
4	**1**	V78K	(*R*)-**2**	98	95
5	**1**	F87A	(*R*)-**2**	98	6
6	**1**	F87L	(*R*)-**2**	99	99
7	**1**	F87R	(*R*)-**2**	97	94
8	**1**	F87S	(*S*)-**2**	98	36
9	**1**	F87T	(*S*)-**2**	99	34
10	**1**	T88Y	(*R*)-**2**	99	95
11	**1**	A328F	(*S*)-**2**	89	6
12	**1**	A328H	(*R*)-**2**	99	98
13	**1**	F87S/A328F	(*S*)-**2**	91	94
14	**1**	F87T/A328F	(*S*)-**2**	91	96
15	**3**	WT	(*S*)-**4**	99	88
16	**3**	V78F	(*S*)-**4**	99	89
17	**3**	V78W	(*S*)-**4**	99	92
18	**3**	F87A	(*S*)-**4**	99	10
19	**3**	F87G	(*R*)-**4**	93	34
20	**3**	T268 K	(*S*)-**4**	99	89
21	**3**	A328R	(*R*)-**4**	98	76

[a]Kinetic parameters were measured for the most enantioselective mutants. Values were obtained by averaging at least three independent experiments performed at 15 mM.

enhance reversal of enantioselectivity, two different mutants were constructed by combining mutations from the best *S*-selective variants: F87S or F87T with A328F. The resulting variants showed more than a purely additive[16] boost in *S*-enantioselectivity without compromising regioselectivity (94−96% ee; Table 1, entries 13 and 14).

We then tested the 28 mutants that showed measurable activity toward substrate **1** (Supporting Information, Table S1) and WT in the hydroxylation of ketone **3**. Only six of these led to excellent regioselectivity and moderate to good enantioselectivity (Table 1, entries 16−21). WT P450-BM3 is highly selective for formation of (*S*)-**4** (88%). We observe that the V78W mutant has increased enantioselectivity (92%) over WT in favor of (*S*)-**4**, while A328R displays the highest ee (76%) with preferential formation of (*R*)-**4**.

Kinetic parameters TOF (turnover number frequency) and TTN (total turnover number) were determined for the most enantioselective mutants used in the formation of **2** and **4**, which show that these mutants are highly active on this type of substrate (Table 2). The results set the stage for future bioprocess optimization.

Table 2. Kinetic Parameters for Oxidative Hydroxylation of Ketones 1 and 3[a]

entry	substrate	P450-BM3	product	TOF[b]	TTN[c]
1	**1**	WT[d]	(*R*)-**2**	24.1	863
2	**1**	F87L	(*R*)-**2**	32.8	1964
3	**1**	F87T/A328F	(*S*)-**2**	16.6	1469
4	**3**	WT[d]	(*S*)-**4**	9.5	1406
5	**3**	V78W	(*S*)-**4**	11.4	1400
6	**3**	A328R	(*R*)-**4**	4.3	355

[a]Catalyzed by the most enantioselective P450-BM3 mutants from Table 1. Values were obtained by averaging at least three independent experiments at 75 000 nmol. [b]TOF (turnover number frequency) is given in nanomoles of product per nanomole of protein per minute. [c]TTN (total turnover number) is given in nanomoles of product per nanomole of protein at the end of reaction. [d]Kinetic parameters of WT P450-BM3 are indicated for comparison.

In order to expand the substrate scope, we subjected several substituted propiophenones **5**−**9** and benzyl methyl ketones **10**−**14** to oxidative hydroxylation by WT P450-BM3 and some of the mutants previously evolved for **1**. Chart 1 shows that for most substrates (the exception being **9**), both *R*- and *S*-selective mutants were observed. As found for substrate **1**, the F87L mutant is *R*-enantioselective (93−99%) for reaction with propiophenones **5**−**9** but also very *S*-selective for benzyl methyl ketones **10** and **11** (94% and 96%, respectively). As is the case for substrate **3**, only low amounts of enantioselectivity (20−46%) were achieved for *R*-hydroxylation of **11**−**14** with the F87G mutant. Conversely, a very high ee (96%) is measured for the same mutant with substrate **10**.

Docking and MD simulations were performed for **1** with WT P450-BM3 and the F87T/A328F mutant to rationalize the observed (opposite) selectivities. Docking calculations alone were performed for substrate **3** with the WT and A328R mutant (Supporting Information, Figure S2).

Hydroxylation of aliphatic C−H bonds in P450 enzymes is widely accepted to occur via the radical rebound mechanism.[12] Hence it is assumed that the abstraction of the pro-*R* and pro-*S* hydrogen atoms from **1** will result in formation of (*R*)-**2** and (*S*)-**2**, respectively. The hydrogen atom of the substrate that spends the largest amount of time in a position close enough to react with the catalytically active Fe^{V}=O moiety is used as the main determinant of selectivity.

The shapes of the active-site pockets of the WT and F87T/A328F mutants promote the formation of (*R*)-**2** and (*S*)-**2**, respectively (Figure 1). The phenyl ring of the substrate forms a π-stacking interaction with a phenylalanine side chain. This interaction is formed with F87 in the WT and with F328,

dx.doi.org/10.1021/jo502397s | J. Org. Chem. 2015, 80, 950−956

Chart 1. Products of α-Hydroxylation of Ketones[a,b]

	(*R*)-**5**	(*R*)-**6**	(*R*)-**7**	(*R*)-**8**	(*R*)-**9**
WT	89% regio, 97% ee	83% regio, 98% ee	95% regio, 94% ee	99% regio, 92% ee	97% regio, 95% ee
F87L	91% regio, 98% ee	87% regio, 99% ee	99% regio, 98% ee	99% regio, 93% ee	99% regio, 97% ee
	(*S*)-**5**	(*S*)-**6**	(*S*)-**7**	(*S*)-**8**	— [a]
F87T/A328F	84% regio, 96% ee	89% regio, 96% ee	99% regio, 96% ee	96% regio, 82% ee	
	(*R*)-**10**	(*R*)-**11**	(*R*)-**12**	(*R*)-**13**[b]	(*R*)-**14**
F87G	62% regio, 96% ee	91% regio, 46% ee	95% regio, 45% ee	99% regio, 27% ee	96% regio, 20% ee
	(*S*)-**10**	(*S*)-**11**	(*S*)-**12**	(*S*)-**13**[b]	(*S*)-**14**
WT	4% regio, 91% ee	75% regio, 94% ee	92% regio, 85% ee	89% regio, 69% ee	86% regio, 65% ee
F87L	81% regio, 94% ee	86% regio, 96% ee			T268K 92% regio, 72% ee

[a]No *S*-selective mutant was found for **9**. [b]Absolute configuration assignment was done by comparing the optical rotation signs with **9**–**11**. Activity of WT and of the best mutants for all substrates is comparable with TOF numbers for hydroxylation of **1** and **3**.

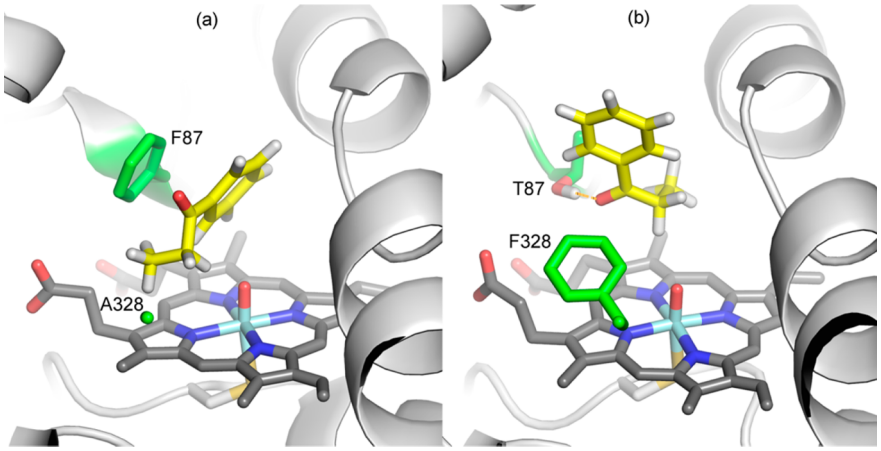

Figure 1. Binding positions of substrate **1** in (a) WT P450-BM3 and (b) F87T/A328F mutant from MD simulations, consistent with formation of (*R*)-**2** and (*S*)-**2**, respectively.

located on the opposite side of the binding pocket, in the F87T/A328F mutant. In the F87T/A328F mutant, the carbonyl oxygen of **1** interacts with the hydroxyl group of T87.

Docking poses for substrate **3** in the WT and A328R mutant are consistent with the observed selectivity (see Supporting Information). In the A328R mutant, a hydrogen-bonding interaction is observed between the carbonyl oxygen of **3** and the side chain of R328, as well as a π-stacking interaction with F87. These two interactions put this substrate in a position where the pro-*R* hydrogen atom is closest to the heme iron. In the WT a different binding orientation of **3** is observed in which the phenyl ring of the substrate forms a closer π-stacking interaction with F87, the pro-*S* hydrogen then being closest to the heme iron.

CONCLUSIONS

In summary, we have developed an asymmetric biocatalytic route to chiral acyloins based on the regio- and enantioselective P450-BM3-catalyzed oxidative hydroxylation of ketones. The use of this class of compounds as starting materials for acyloin synthesis has been reported previously employing chiral synthetic catalysts[2,3] but not biocatalysts such as P450

dx.doi.org/10.1021/jo502397s | J. Org. Chem. 2015, 80, 950–956

monooxygenases.[17] Thus, the present contribution expands the toolbox of organic chemists, while widening the substrate range of P450 enzymes. Structure-based directed evolution[14,15] was applied to enhance and to invert enantioselectivity, a strategy that can be used in future studies when targeting other ketones.

EXPERIMENTAL SECTION

Biology. *General Information.* The reagents used have been described previously elsewhere.[18] *Escherichia coli* BOU730 cells [an *E. coli* strain derived from BL21(DE3) that contains a copy of *gdh* gene from *B. megaterium* under the control of T7 promoter][18a] were used during this study. Electrocompetent cells were prepared in-house according to standard protocols.[19]

Library Creation. Libraries V78-T88 (library A), V78-L181 (library B), and T268-A328 (library C) were created by use of a reduced amino acid alphabet randomization scheme, and library D (F87) was created by saturation mutagenesis at that position, as previously reported.[18b]

P450-BM3 Mutant Screening. Screening of the P450-BM3 variants created by mutagenic PCR was performed by gas chromatography (GC), as described previously.[18] Single BOU730 cell colonies containing the P450-BM3 variants grown in the presence of kanamycin (kan, 50 μM) were inoculated into 96-deep-well plates [each well containing lysogeny broth (LB) (800 μL) and kan (50 μg/mL)] during 5 h at 37 °C. An aliquot of this culture (100 μL) was added to a 96-deep-well plate [each well containing terrific broth (TB) (900 μL), kan (50 μg/mL), and isopropyl β-thiogalactoside (IPTG; 0.2 mM)] and incubated at 30 °C for 20 h. Cells were then centrifuged (4000 rpm, 15 min at 4 °C), the supernatant was discarded, and the pellets were resuspended in lysis buffer [each well containing 500 μL of phosphate buffer (pH 7.4, 100 mM), lysozyme (14 mg/mL), and DNase I (6 units/mL)]. Plates were incubated for 45 min at 37 °C and centrifuged at 4000 rpm for 30 min at 4 °C. An aliquot of the resulting supernatant (350 μL) was transferred to a new 96-deep-well plate containing 150 μL of reaction buffer [phosphate buffer (pH 7.4, 100 mM), glucose (100 mM), and nicotinamide adenine dinucleotide phosphate ($NADP^+$, 250 μM)]. Reaction was started by addition of **1** (final concentration 15 mM, 7.5 μmol) and incubated at 25 °C for 20 h. After incubation, samples were extracted with ethyl acetate (400 μL) and subjected to chiral GC analysis: column Ivadex 1, 25 m; i.d. 0.25 mm; pressure 1.0 bar H_2; injector 230 °C; oven temperature gradient 50−124 (3 °C/min ramp), 124−220 (25 °C/min ramp); 1 μL; 99:1; FID detector 350 °C.

Small-Scale Reactions. The most enantioselective P450-BM3 mutants for **2** found during the initial screening were sequenced and grown to perform small-scale reactions. Transformed BOU730 cells were grown and the best mutants (Table S1, Supporting Information) were overexpressed in TB (50 mL) as described previously.[18] Cell cultures were split into 2 mL aliquots and centrifuged, and the resulting pellets were stored at −80 °C for further use. Small-scale biohydroxylation reactions were performed by resuspending aliquots in 500 μL of lysis buffer [phosphate buffer (pH 7.4, 100 mM), lysozyme (14 mg/mL), and DNase I (6 units/mL)] and incubated for 45 min at 37 °C. Reactions were then centrifuged (15 min, 10 000 rpm at room temperature) and 445 μL of supernatant were transferred to a new 1.5 mL tube containing 50 μL of glucose (100 mM final concentration) and 5 μL of $NADP^+$ (250 μM final concentration). Reaction was started by addition of 1 μL of the corresponding starting material **1**, **3**, or **5**−**14** (9−15 mM, 4.5−7.5 μmol) and incubated at 25 °C (900 rpm) for 20 h. Samples were extracted with ethyl acetate (500 μL) and subjected to GC analysis by the measuring methods described below.

In most cases, small amounts of tautomerized products were observed, a process that depends on the reaction time and the mutant used. Partial tautomerization of acyloins is a common phenomenon.[20]

Turnover Number Determination. Calculation of the kinetic parameters TOF (turnover number frequency) and TTN (total turnover number) was done as described previously.[18b] Cultures of BOU730 cells overexpressing the corresponding variants of P450-BM3 in TB (400 mL, kan 50 μg/mL) were split in Falcon tubes (25 mL aliquots) and centrifuged for 7 min at 4000 rpm at room temperature. The supernatant was discarded and the pellet was resuspended in 5 mL of reaction buffer [phosphate buffer (pH 7.4, 100 mM), glucose (100 mM), and $NADP^+$ (200 μM)]. Biotransformation was started by addition of **1** or **3** (15 mM, 75 000 nmol). Reactions were carried out in an Erlenmeyer flask (100 mL) at 30 °C with mild agitation. Aliquots (500 μL) were harvested at different time points (20, 60, 120, 180, 240, and 1200 min), extracted with ethyl acetate (500 μL), and subjected to GC analysis. TOFs were calculated on the basis of substrate consumption (based on GC results) during the time in which the highest substrate consumption rate was observed (first 20 min of reaction). TTNs were calculated at the time point in which maximum conversion was achieved. All reactions were done in parallel and in triplicate. Concentration of P450-BM3 variants was measured in triplicate as previously described.[21] Values obtained varied from 2 to 2.5 μM.

Chemistry. *General Remarks.* Starting compounds were purchased and used without further purification. Phenylacetone was prepared by a described procedure.[22] NMR spectra were recorded on a 300 MHz (^{1}H, 300 MHz; ^{13}C, 75 MHz) spectrometer with tetramethylsilane (TMS) as internal standard (δ = 0), unless otherwise noted. Conversion and enantiomeric excess were determined by achiral and chiral gas chromatography.

Compound Characterization. All reactions were scaled up (100 mg of starting material approximately) with WT-P450 and P450 mutants, in order to obtain enough material for NMR characterization (chemical or bioprocess optimization was not performed). Products were then purified by column chromatography. They were identified by NMR spectroscopy and compared with authentic samples as described previously in the respective literature.

(R)-(+)-2-Hydroxy-1-phenylpropan-1-one ***2****.*

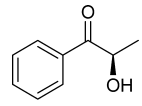

The absolute configuration of (*R*)-**2** was assigned by comparison with an authentic sample as reported by Luczak and co-workers.[23] The residue was purified by column chromatography (SiO_2, ethyl acetate/petroleum ether 1:4). White crystals, 12% yield (13 mg); ^{1}H NMR (300 MHz, $CDCl_3$) δ 7.93 (d, ^3J = 8.2 Hz, 2H), 7.63 (t, ^3J = 7.4 Hz, 1H), 7.51 (t, ^3J = 7.7 Hz, 2H), 5.17 (m, 1H), 3.79 (d, ^3J = 6.3 Hz, 1H), 1.45 (d, ^3J = 7.0 Hz, 3H); ^{13}C NMR (75 MHz, $CDCl_3$) δ 202.3, 133.9, 133.3, 128.8 (2C), 128.6 (2C), 69.3, 22.2; $[\alpha]_D^{20}$ = +58.8 (*c* 0.83, $CHCl_3$), lit. (*R*)-(+)-**2** $[\alpha]_D^{20}$ = +55.4 (*c* 0.1, $CHCl_3$);[23] ee = 99%.

(S)-(+)-1-Hydroxy-1-phenylpropan-2-one ***4****.*

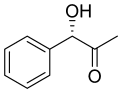

The absolute configuration of (*S*)-**4** was assigned by comparison with an authentic sample as reported by Schwarz and Meyers.[24] The residue was purified by column chromatography (SiO_2, ethyl acetate/petroleum ether 1:4). Colorless liquid, 4% yield (4.4 mg); ^{1}H NMR (300 MHz, $CDCl_3$) δ 7.29 (m, 5H), 5.03 (d, ^3J = 4.0 Hz, 1H), 4.23 (d, ^3J = 4.2 Hz, 1H), 2.02 (s, 3H); ^{13}C NMR (75 MHz, $CDCl_3$) δ 207.1, 138.1, 129.1, 128.8 (2C), 127.5 (2C), 80.3, 25.3; ee = 92%.

(R)-(+)-2-Hydroxy-1-(p-tolyl)propan-1-one ***5****.*

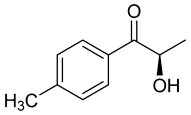

The absolute configuration of (*R*)-**5** was assigned by comparison with an authentic sample as reported by Tsuchihashi and co-workers.[25] The residue was purified by column chromatography (SiO_2, ethyl acetate/petroleum ether 1:4). White solid, 23% yield (24.4 mg); ^{1}H NMR (300 MHz, $CDCl_3$) δ 7.82 (d, *J* = 8.0 Hz, 2H), 7.29 (d, *J* = 8.0 Hz, 2H), 5.12 (q, *J* = 7.0 Hz, 1H), 3.70 (br s, 1H, OH), 2.42 (s, 3H),

dx.doi.org/10.1021/jo502397s | J. Org. Chem. 2015, 80, 950−956

1.43 (d, J = 7.0 Hz, 3H); ^{13}C NMR (75 MHz, $CDCl_3$) δ 202.0, 145.1, 130.8, 129.6 (2C), 128.8 (2C), 69.2, 22.5, 21.8; ee = 98%.

(R)-(+)-2-Hydroxy-1-(4-methoxyphenyl)propan-1-one ***6***.

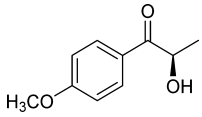

The absolute configuration of (*R*)-**6** was assigned by comparison with an authentic sample as reported by Luczak and co-workers.[23] The residue was purified by column chromatography (SiO_2, ethyl acetate/petroleum ether 1:2). Pale yellow oil, 7% yield (8.4 mg); ^{1}H NMR (300 MHz, $CDCl_3$) δ 7.91 (d, J = 9.0 Hz, 2H), 6.96 (d, J = 9.0 Hz, 2H), 5.10 (q, J = 7.0 Hz, 1H), 3.88 (s, 3H), 3.54 (br s, 1H), 1.44 (d, J = 7.0 Hz, 3H); ^{13}C NMR (75 MHz, $CDCl_3$) δ 200.8, 164.3, 131.1, 126.2, 114.2, 69.0, 55.6, 22.7; ee = 99%.

(R)-(+)-1-(4-Chlorophenyl)-2-hydroxypropan-1-one ***7***.

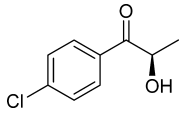

The absolute configuration of (*R*)-**7** was assigned by comparison with an authentic sample as reported by Müller and co-workers.[26] The residue was purified by column chromatography (SiO_2, ethyl acetate/petroleum ether 1:2). Pale yellow crystals, 18% yield (19.7 mg); ^{1}H NMR (300 MHz, $CDCl_3$) δ 7.80 (d, J = 8.8 Hz, 2H), 7.40 (d, J = 8.8 Hz, 2H), 5.05 (q, J = 7.0 Hz, 1H), 3.81 (br s, 1H), 1.37 (d, J = 7.0 Hz, 3H); ^{13}C NMR (75 MHz, $CDCl_3$) δ 201.3, 140.6, 131.8, 130.1 (2C), 129.3 (2C), 69.4, 22.2; ee = 98%.

(R)-(+)-1-(4-Bromophenyl)-2-hydroxypropan-1-one ***8***.

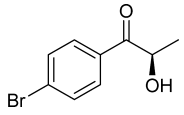

The absolute configuration of (*R*)-**8** was assigned by comparison with an authentic sample as reported by Müller and co-workers.[26] The residue was purified by column chromatography (SiO_2, ethyl acetate/petroleum ether 1:2). Colorless crystals, 4% yield (4 mg); ^{1}H NMR (300 MHz, $CDCl_3$) δ 7.73 (d, J = 8.7 Hz, 2H), 7.58 (d, J = 8.7 Hz, 2H), 5.04 (q, J = 7.0 Hz, 1H), 3.65 (br s, 1H), 1.37 (d, J = 7.0 Hz, 3H); ^{13}C NMR (75 MHz, $CDCl_3$) δ 201.5, 132.4 (2C), 132.2, 130.2 (2C), 129.3, 69.4, 22.3; ee = 93%.

(R)-(+)-1-(2-Fluorophenyl)-2-hydroxypropan-1-one ***9***.

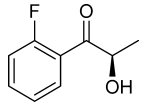

The absolute configuration of (*R*)-**9** was assigned by comparison with an authentic sample as reported by Müller and co-workers.[26] The residue was purified by column chromatography (SiO_2, ethyl acetate/petroleum ether 1:4). Pale yellow viscous oil, 24% yield (30 mg); ^{1}H NMR (300 MHz, $CDCl_3$) δ 7.95–7.78 (m, 1H), 7.56–7.48 (m, 1H), 7.22 (td, J = 7.8, 1.0 Hz, 1H), 7.13–7.06 (m, 1H), 4.98 (qd, J = 7.0, 2.8 Hz, 1H), 3.58 (br s, 1H, OH), 1.33 (dd, J = 7.0, 1.5 Hz, 3H); ^{13}C NMR (75 MHz, $CDCl_3$) δ 201.0 (d, J = 4.4 Hz, 1C), 161.7 (d, J = 255.4 Hz, 1C), 135.6 (d, J = 9.2 Hz, 1C), 131.23 (d, J = 2.8 Hz, 1C), 124.9 (d, J = 3.3 Hz, 1C), 122.3 (d, J = 13.4 Hz, 1C), 116.8 (d, J = 23.6 Hz, 1C), 72.8 (d, J = 9.2 Hz, 1C), 20.8 (d, J = 1.1 Hz, 1C); ee = 97%.

(S)-(+)-1-Hydroxy-1-(p-tolyl)propan-2-one ***10***.

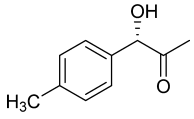

The absolute configuration of (*S*)-**10** was assigned by comparison with an authentic sample as reported by Fleming et al.[27] The residue was purified by column chromatography (SiO_2, ethyl acetate/petroleum ether 1:4). Pale yellow crystals, 26% yield (28.3 mg); ^{1}H NMR (300 MHz, $CDCl_3$) δ 7.12 (s, 4H), 4.98 (s, 1H), 3.62 (br s, 1H), 2.27 (s, 3H), 1.99 (s, 3H); ^{13}C NMR (75 MHz, $CDCl_3$) δ 207.4, 138.7, 135.1, 129.8 (2C), 127.4 (2C), 80.0, 25.3, 21.2; ee = 94%.

(S)-(+)-1-Hydroxy-1-(4-methoxyphenyl)propan-2-one ***11***.

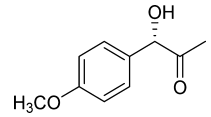

The absolute configuration of (*S*)-**11** was assigned by comparison with an authentic sample as reported by Watson and co-workers.[28] The residue was purified by column chromatography (SiO_2, ethyl acetate/petroleum ether 1:4). Pale yellow crystals, 8% yield (9 mg); ^{1}H NMR (300 MHz, $CDCl_3$) δ 7.22 (d, J = 8.6 Hz, 2H), 6.90 (d, J = 8.6 Hz, 2H), 5.04 (s, 1H), 3.80 (s, 3H), 2.06 (s, 3H); ee = 96%.

(S)-(+)-1-(4-Chlorophenyl)-1-hydroxypropan-2-one ***12***.

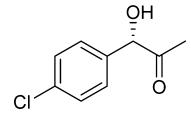

The absolute configuration of (*S*)-**12** was assigned by comparison with an authentic sample as reported by Yang and co-workers.[29] The residue was purified by column chromatography (SiO_2, ethyl acetate/petroleum ether 1:2). Pale yellow crystals, 29% yield (36.7 mg); ^{1}H NMR (300 MHz, $CDCl_3$) δ 7.30 (d, J = 8.6 Hz, 2H), 7.20 (d, J = 8.6 Hz, 2H), 5.00 (s, 1H), 2.01 (s, 3H); ^{13}C NMR (75 MHz, $CDCl_3$) δ 206.6, 136.6, 134.8, 129.3 (2C), 128.8 (2C), 79.5, 25.3; ee = 85%.

(S)-(+)-1-(4-Bromophenyl)-1-hydroxypropan-2-one ***13***.

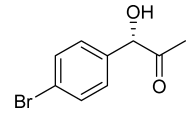

The absolute configuration of (*S*)-**13** was assigned by comparing the optical rotation signs with **10**–**12**. The residue was purified by column chromatography (SiO_2, ethyl acetate/petroleum ether 1:4). Pale yellow crystals, 56% yield (60 mg); ^{1}H NMR (300 MHz, $CDCl_3$) δ 7.52 (d, J = 8.4 Hz, 2H), 7.21 (d, J = 8.4 Hz, 2H), 5.05 (s, 1H), 2.08 (s, 3H); ^{13}C NMR (75 MHz, $CDCl_3$) δ 206.5, 137.1, 132.3 (2C), 129.1 (2C), 122.9, 79.6, 25.3; ee = 69%.

(S)-(+)-1-(2-Fluorophenyl)-1-hydroxypropan-2-one ***14***.

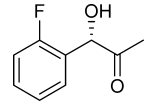

The absolute configuration of (*S*)-**14** was assigned by comparison with an authentic sample as reported by Turner and co-workers.[30] The residue was purified by column chromatography (SiO_2, ethyl acetate/petroleum ether 1:5). Pale yellow viscous oil, 43% yield (48 mg); ^{1}H NMR (300 MHz, $CDCl_3$) δ 7.31–7.18 (m, 2H), 7.14–6.97 (m, 2H), 5.34 (s, 1H), 3.88 (br s, 1H), 2.05 (d, J = 0.7 Hz, 3H); ^{13}C NMR (75 MHz, $CDCl_3$) δ 205.1 (d, J = 1.2 Hz, 1C), 159.3 (d, J = 247.1 Hz, 1C), 129.3 (d, J = 8.3 Hz, 1C), 127.7 (d, J = 3.6 Hz, 1C), 124.2 (d, J = 13.6 Hz, 1C), 123.7 (d, J = 3.6 Hz, 1C), 114.8 (d, J = 21.6 Hz, 1C), 72.6 (d, J = 3.4 Hz, 1C), 23.9 (d, J = 2.3 Hz, 1C); ee = 65%.

Molecular Docking Calculations: Details of Docking and Molecular Dynamics Simulations. Docking calculations were performed with the AUTODOCK VINA[31] program within the PyMol interface.[32] The structures of substrates **1** and **2** were built in the Maestro program,[33] and a geometry optimization was performed by use of the ORCA program (version 3.0.1) at the BP86/SV level.[34]

Preliminary simulations were performed starting from the 1BU7 crystal structure. However, in this structure the substrate (**1**) failed to remain in the active site. The 1JPZ crystal structure[35] contains a cocrystallized ligand (*N*-palmitoylglycine) and hence has a larger active site cavity than the 1BU7 structure. This ligand was removed prior to docking and MD simulations. When the 1JPZ crystal structure was used, the substrate remained in the active site for the entirety of the simulations. Mutations were performed within PyMol, and the

dx.doi.org/10.1021/jo502397s | J. Org. Chem. 2015, 80, 950–956

conformations of mutated residues were selected such to minimize steric clashes.

For each MD simulation, the protein was solvated and neutralized with the *tleap* program in a truncated octahedron water box of sufficient size to provide a solvent layer of a minimum of 12 Å thickness surrounding the protein. The simulation system was neutralized by the addition of Na^+ ions. Molecular dynamics simulations were performed with the Amber12 program[36] with the FF12SB molecular mechanics force field[37] and TIP4P-EW water model.[38] Molecular mechanics parameters for the cysteine-coordinated heme in the Compound I state were obtained from ref 39. The parameters and topology of substrate **1** were obtained by use of the ANTECHAMBER program with the generalized Amber force field (GAFF).

The minimization and equilibration procedure for the relaxation of each system prior to production-phase simulations was the same as described previously.[40] Two unrestrained 24 ns NPT simulations were performed on the selected docking poses for both the WT and F87T/A328F mutant.

For the F87T/A328F mutant, two 12 ns simulations were first performed on the substrate-free mutant prior to docking, in order to allow the protein to relax in the presence of the mutated residues. The structures from the two simulations were then clustered in the *cpptraj* program. Clustering was performed on the basis of the positions of residues lining the active-site cavity (residues 75, 78, 82, 87, 88, 177, 181, 260, 263, 264, 267, 268, 328, 437, and 438). Six clusters were obtained by use of the *average-linkage* algorithm. Prior to clustering, all water molecules were removed. The docking of substrate **1** was then performed on the most populated representative structure from the clustering calculation. Following the selection of a docking pose, two 24 ns MD simulations were performed, repeating the solvation, minimization, and equilibration steps as detailed above.

■ ASSOCIATED CONTENT

Supporting Information

Additional text describing detailed results from docking and MD simulations; one table listing P450-BM3 hits found after screening with **1**; seven figures showing randomization sites A–D, docking results for **3**, and RMSD of backbone heavy atoms and distances calculated during MD simulations of **1**; selected NMR spectra and GC chromatograms. This material is available free of charge via the Internet at http://pubs.acs.org/.

■ AUTHOR INFORMATION

Corresponding Author

*E-mail reetz@mpi-muelheim.mpg.de.

Author Contributions

[§]R.A., G.-D.R., R.L., and A.I. contributed equally.

Notes

The authors declare no competing financial interest.

■ ACKNOWLEDGMENTS

Financial support by the Max-Planck-Society and the Arthur C. Cope Foundation is gratefully acknowledged.

■ REFERENCES

(1) Hoyos, P.; Sinisterra, J. V.; Molinari, F.; Alcantara, A. R.; De Maria, P. D. *Acc. Chem. Res.* **2010**, *43*, 288–299.

(2) (a) Davis, F. A.; Chen, B. C. *Chem. Rev.* **1992**, *92*, 919–934. (b) Plietker, B. *Tetrahedron: Asymmetry* **2005**, *16*, 3453–3459. (c) Plietker, B. *Eur. J. Org. Chem.* **2005**, *9*, 1919–1929. (d) Momiyama, N.; Yamamoto, H. *J. Am. Chem. Soc.* **2004**, *126*, 5360–5361.

(3) (a) Brown, S. P.; Brochu, M. P.; Sinz, C. J.; MacMillan, D. W. C. J. *Am. Chem. Soc.* **2003**, *125*, 10808–10809. (b) Bogevig, A.; Sunden, H.; Cordova, A. *Angew. Chem., Int. Ed.* **2004**, *43*, 1109–1112. (c) Hayashi, Y.; Yamaguchi, J.; Sumiya, T.; Shoji, M. *Angew. Chem., Int. Ed.* **2004**, *43*, 1112–1115.

(4) (a) Enders, D.; Kallfass, U. *Angew. Chem., Int. Ed.* **2002**, *41*, 1743–1745. (b) Marti, J.; Castells, J.; Lopez-Calahorra, F. *Tetrahedron Lett.* **1993**, *34*, 521–524.

(5) (a) Zhang, J. D.; Xu, T. T.; Li, Z. *Adv. Synth. Catal.* **2013**, *355*, 3147–3153. (b) Onomura, O.; Arimoto, H.; Matsumura, Y.; Demizu, Y. *Tetrahedron Lett.* **2007**, *48*, 8668–8672.

(6) (a) Drauz, K., Gröger, H., May, O., Eds. *Enzyme Catalysis in Organic Chemistry*, 3rd ed.; Wiley–VCH: Weinheim, Germany, 2012. (b) Perspective on enzymes in organic chemistry: Reetz, M. T. *J. Am. Chem. Soc.* **2013**, *135*, 12480–12496.

(7) (a) Müller, M.; Gocke, D.; Pohl, M. *FEBS J.* **2009**, *276*, 2894–2904. (b) Hischer, T.; Gocke, D.; Fernandez, M.; Hoyos, P.; Alcantara, A. R.; Sinisterra, J. V.; Hartmeier, W.; Ansorge-Schumacher, M. B. *Tetrahedron* **2005**, *61*, 7378–7383. (c) Dominguez de Maria, P.; Stillger, T.; Pohl, M.; Kiesel, M.; Liese, A.; Gröger, H.; Trauthwein, H. *Adv. Synth. Catal.* **2008**, *350*, 165–173. (d) Westphal, R.; Vogel, C.; Schmitz, C.; Pleiss, J.; Müller, M.; Pohl, M.; Rother, D. *Angew. Chem., Int. Ed.* **2014**, *53*, 9376–9379.

(8) Recent examples of reductase-catalyzed reactions of 1,2-diketones: (a) Bel-Rhlid, R.; Fauve, A.; Veschambre, H. *J. Org. Chem.* **1989**, *54*, 3221–3223. (b) Hoyos, P.; Sansottera, G.; Fernandez, M.; Molinari, F.; Sinisterra, J. V.; Alcantara, A. R. *Tetrahedron* **2008**, *64*, 7929–7936. (c) Demir, A. S.; Ayhan, P.; Demirtaş, U.; Erkılıç, U. *J. Mol. Catal. B: Enzym.* **2008**, *55*, 164–168.

(9) Examples of oxidase-catalyzed reactions of 1,2-diols: (a) Bortolini, O.; Casanova, E.; Fantin, G.; Medici, A.; Poli, S.; Hanau, S. *Tetrahedron: Asymmetry* **1998**, *9*, 647–651. (b) Molinari, F. *Curr. Org. Chem.* **2006**, *10*, 1247–1263.

(10) (a) Adam, W.; Diaz, M. T.; Fell, R. T.; Saha-Möller, C. R. *Tetrahedron: Asymmetry* **1996**, *7*, 2207–2210. (b) Hoyos, P.; Fernandez, M.; Sinisterra, J. V.; Alcantara, A. R. *J. Org. Chem.* **2006**, *71*, 7632–7637. (c) Hoyos, P.; Dominguez de Maria, P.; Sinisterra, J. V.; Alcantara, A. R. *Hydrolase based synthesis of enantiopure R-hydroxy ketones: From racemic resolutions to chemo-enzymatic dynamic kinetic resolutions.* ; Biotechnology Research: Technology and Applications; Nova Science Publishers, Inc.: New York, 2009; pp 97–119. (d) Tanyeli, C.; Akhmedov, I.; Iyigun, C. *Tetrahedron: Asymmetry* **2006**, *17*, 1125–1128. (e) Scheid, G.; Ruijter, E.; Konarzycka-Bessler, M.; Bornscheuer, U. T.; Wessjohann, L. A. *Tetrahedron: Asymmetry* **2004**, *15*, 2861–2869. (f) Ödman, P.; Wessjohann, L. A.; Bornscheuer, U. T. *J. Org. Chem.* **2005**, *70*, 9551–9555. (g) Petrenz, A.; Dominguez de Maria, P.; Ramanathan, A.; Hanefeld, U.; Ansorge-Schumacher, M. B.; Kara, S. *J. Mol. Catal. B: Enzym.* **2015**, *396*, 328–334.

(11) (a) Bogar, K.; Hoyos Vidal, P.; Alcantara Leon, A. R.; Bäckvall, J.-E. *Org. Lett.* **2007**, *9*, 3401–3404. (b) de Gonzalo, G.; Torress Pazmino, D. E.; Ottolina, G.; Fraaije, M. W.; Carrea, G. *Tetrahedron: Asymmetry* **2005**, *16*, 3077–3083.

(12) Reviews of P450 monooxygenases: (a) Ortiz de Montellano, P. R. *Cytochrome P450: Structure, Mechanism, and Biochemistry*, 3rd ed.; Springer: Berlin, 2005. (b) Isin, E. M.; Guengerich, F. P. *Biochim. Biophys. Acta, Gen. Subj.* **2007**, *1770*, 314–329. (c) Ortiz de Montellano, P. R. *Chem. Rev.* **2010**, *110*, 932–948. (d) Whitehouse, C. J. C.; Bell, S. G.; Wong, L.-L. *Chem. Soc. Rev.* **2012**, *41*, 1218–1260. (e) O'Reilly, E.; Köhler, V.; Flitsch, S. L.; Turner, N. J. *Chem. Commun.* **2011**, *47*, 2490–2501. (f) Fasan, R. *ACS Catal.* **2012**, *2*, 647–666. (g) Khatri, Y.; Hannemann, F.; Girhard, M.; Kappl, R.; Meme, A.; Ringle, M.; Janocha, S.; Leize-Wagner, E.; Urlacher, V. B.; Bernhardt, R. *Biotechnol. Appl. Biochem.* **2013**, *60*, 18–29. (h) Holtmann, D.; Fraaije, M. W.; Arends, I. W. C. E.; Opperman, D. J.; Hollmann, F. *Chem. Commun.* **2014**, *50*, 13180–13200. (i) Yamazaki, H. *Fifty Years of Cytochrome P450 Research*; Springer: Berlin, 2014. (j) Roiban, G.-D.; Reetz, M. T. *Chem. Commun.* **2015**, DOI: 10.1039/C4CC09218J.

(13) (a) Narhi, L. O.; Fulco, A. J. *J. Biol. Chem.* **1986**, *261*, 7160–7169. (b) Munro, A. W.; Leys, D. J.; McLean, K. J.; Marshall, K. R.; Ost, T. W. B.; Daff, S.; Miles, C. S.; Chapman, S. K.; Lysek, D. A.; Moser, C. C.; Page, C. C.; Dutton, P. L. *Trends Biochem. Sci.* **2002**, *27*, 250–257. (c) Jovanovic, T.; Farid, R.; Friesner, R. A.; McDermott, A. E. *J. Am. Chem. Soc.* **2005**, *127*, 13548–13552. (d) Clodfelter, K. H.;

Waxman, D. J.; Vajda, S. *Biochemistry* **2006**, *45*, 9393−9407. (e) Schwaneberg, U.; Sprauer, A.; Schmidt-Dannert, C.; Schmid, R. D. *J. Chromatogr. A* **1999**, *848*, 149−159.
(14) Reviews of directed evolution: (a) *Directed Evolution Library Creation*, 2nd ed.; Gillam, E. M. J., Copp, J. N., Ackerley, D. F., Eds.; Methods in Molecular Biology; Humana Press: Totowa, NJ, 2014. (b) Widersten, M. *Curr. Opin. Chem. Biol.* **2014**, *21*, 42−47. (c) Siloto, R. M. P.; Weselake, R. J. *Biocatal. Agric. Biotechnol.* **2012**, *1*, 181−189. (d) Goldsmith, M.; Tawfik, D. S. *Curr. Opin. Struct. Biol.* **2012**, *22*, 406−412. (e) Cobb, R. E.; Chao, R.; Zhao, H. *AIChE J.* **2013**, *59*, 1432−1440. (f) Reetz, M. T. Directed evolution of enzymes. In *Enzyme Catalysis in Organic Synthesis*; Drauz, K., Dröge, H., May, O., Eds.; Wiley−VCH: Weinheim, Germany, 2012; Vol. *1*, pp 119−190. (g) Bommarius, A. S.; Blum, J. K.; Abrahamson, M. J. *Curr. Opin. Chem. Biol.* **2011**, *15*, 194−200. (h) Quin, M. B.; Schmidt-Dannert, C. *ACS Catal.* **2011**, *1*, 1017−1021. (i) Brustad, E. M.; Arnold, F. H. *Curr. Opin. Chem. Biol.* **2011**, *15*, 201−210. (j) Jäckel, C.; Hilvert, D. *Curr. Opin. Biotechnol.* **2010**, *21*, 753−759. (k) Turner, N. J. *Nat. Chem. Biol.* **2009**, *5*, 567−573. (l) Lutz, S.; Bornscheuer, U. T. *Protein Engineering Handbook*, Vol. *1*−*2*; Wiley−VCH: Weinheim, Germany, 2009.
(15) Review of directed evolution of enantioselective enzymes with emphasis on iterative saturation mutagenesis: Reetz, M. T. *Angew. Chem., Int. Ed.* **2011**, *50*, 138−174.
(16) Review of additive versus nonadditive mutational effects in protein engineering: Reetz, M. T. *Angew. Chem., Int. Ed.* **2013**, *52*, 2658−2666.
(17) P450-catalyzed α-hydroxylation of phenylacetic acid esters: Landwehr, M.; Hochrein, L.; Otey, C. R.; Kasrayan, A.; Bäckvall, J.-E.; Arnold, F. H. *J. Am. Chem. Soc.* **2006**, *128*, 6058−6059.
(18) (a) Agudo, R.; Roiban, G.-D.; Reetz, M. T. *ChemBioChem* **2012**, *13*, 1465−1473. (b) Roiban, G.-D.; Agudo, R.; Reetz, M. T. *Angew. Chem., Int. Ed.* **2014**, *53*, 8659−8663.
(19) Sambrook, J.; Russell, D. W. *The Condensed Protocols from Molecular Cloning: A Laboratory Manual*. Cold Spring Harbor Laboratory Press: New York, 2006.
(20) (a) Perez-Sanchez, M.; Müller, C. R.; Dominguez de Maria, P. *ChemCatChem* **2013**, *5*, 2512−2516. (b) Dominguez de Maria, P.; Stillger, T.; Pohl, M.; Kiesel, M.; Liese, A.; Groger, H.; Trauthwein, H. *Adv. Synth. Catal.* **2008**, *350*, 165−173.
(21) Guengerich, F. P.; Martin, M. V.; Sohl, C. D.; Cheng, Q. *Nat. Protoc.* **2009**, *4*, 1245−1251.
(22) Justik, M. W.; Koser, G. F. *Tetrahedron Lett.* **2004**, *45*, 6159−6163.
(23) Krawczyk, E.; Mielniczak, G.; Owsianik, K.; Luczak, J. *Tetrahedron: Asymmetry* **2012**, *23*, 1480−1489.
(24) Schwarz, J. B.; Meyers, A. I. *J. Org. Chem.* **1998**, *63*, 1619−1629.
(25) Honda, Y.; Ori, A.; Tsuchihashi, G. I. *Bull. Chem. Soc. Jpn.* **1987**, *60*, 1027−1036.
(26) Demir, A. S.; Sesenoglu, O.; Eren, E.; Hosrik, B.; Pohl, M.; Janzen, E.; Kolter, D.; Feldmann, R.; Dunkelmann, P.; Müller, M. *Adv. Synth. Catal.* **2002**, *344*, 96−103.
(27) Fleming, S. A.; Carroll, S. M.; Hirschi, J.; Liu, R. M.; Pace, J. L.; Redd, J. T. *Tetrahedron Lett.* **2004**, *45*, 3341−3343.
(28) Jackson, W. R.; Jacobs, H. A.; Jayatilake, G. S.; Matthews, B. R.; Watson, K. G. *Aust. J. Chem.* **1990**, *43*, 2045−2062.
(29) Jin, M. Y.; Kim, S. M.; Han, H.; Ryu, D. H.; Yang, J. W. *Org. Lett.* **2011**, *13*, 880−883.
(30) Bornemann, S.; Crout, D. H. G.; Dalton, H.; Kren, V.; Lobell, M.; Dean, G.; Thomson, N.; Turner, M. M. *J. Chem. Soc., Perkin Trans. 1 (1972−1999)* **1996**, No. 5, 425−430.
(31) Trott, O.; Olson, A. J. *J. Comput. Chem.* **2010**, *31*, 455−461.
(32) Seeliger, D.; de Groot, B. L. *J. Comput.-Aided Mol. Des.* **2010**, *24*, 417−422.
(33) Maestro v9.6, Schrödinger LLC, 2013.
(34) Neese, F. *Wiley Interdiscip. Rev.: Comput. Mol. Sci.* **2012**, *2*, 73−78.
(35) Haines, D. C.; Tomchick, D. R.; Machius, M.; Peterson, J. A. *Biochemistry* **2001**, *40*, 13456−13465.
(36) Case, D. A.; Darden, T. A.; Cheatham, T. E., III; Simmerling, C. L.; Wang, J.; Duke, R. E.; Luo, R.; Walker, R. C.; Zhang, W.; Merz, K. M.; Roberts, B.; Hayik, S.; Roitberg, A.; Seabra, G.; Swails, J.; Götz, A. W.; Kolossváry, I.; Wong, K. F.; Paesani, F.; Vanicek, J.; Wolf, R. M.; Liu, J.; Wu, X.; Brozell, S. R.; Steinbrecher, T.; Gohlke, H.; Cai, Q.; Ye, X.; Wang, J.; Hsieh, M.-J.; Cui, G.; Roe, D. R.; Mathews, D. H.; Seetin, M. G.; Salomon-Ferrer, R.; Sagui, C.; Babin, V.; Luchko, T.; Gusarov, S.; Kovalenko, A.; Kollman, P. A. *AMBER 12*; University of California, San Francisco, 2012.
(37) Wang, J.; Wolf, R. M.; Caldwell, J. W.; Kollman, P. A.; Case, D. A. *J. Comput. Chem.* **2004**, *25*, 1157−1174.
(38) (a) Horn, H. W.; Swope, W. C.; Pitera, J. W.; Madura, J. D.; Dick, T. J.; Hura, G. L.; Head-Gordon, T. *J. Chem. Phys.* **2004**, *120*, 9665−9678. (b) Horn, H. W.; Swope, W. C.; Pitera, J. W. *J. Chem. Phys.* **2005**, *123*, No. 194504.
(39) Shahrokh, K.; Orendt, A.; Yost, G. S.; Cheatham, T. E. *J. Comput. Chem.* **2012**, *33*, 119−133.
(40) Roiban, G.-D.; Agudo, R.; Ilie, A.; Lonsdale, R.; Reetz, M. T. *Chem. Commun.* **2014**, *50*, 14310−14313.